JACS
JOURNAL OF THE AMERICAN CHEMICAL SOCIETY
Article
pubs.acs.org/JACS

Molecular Design Strategy toward Diarylethenes That Photoswitch with Visible Light

Tuyoshi Fukaminato,*[,†] Takashi Hirose,[‡] Takao Doi,[§] Masaki Hazama,[§] Kenji Matsuda,[‡] and Masahiro Irie*[,∥]

[†]Research Institute for Electronic Science, Hokkaido University, N20, W10, Kita-ku, Sapporo 001-0020, Japan

[‡]Department of Synthetic Chemistry and Biological Chemistry, Graduate School of Engineering, Kyoto University, Katsura, Nishikyo-ku, Kyoto 615-8510, Japan

[§]Department of Chemistry and Biochemistry, Graduate School of Engineering, Kyushu University, Motooka 744, Nishi-ku, Fukuoka 819-0395, Japan

[∥]Department of Chemistry and Research Center for Smart Molecules, Rikkyo University, Nishi-Ikebukuro 3-34-1, Toshima-ku, Tokyo 171-8501, Japan

Supporting Information

ABSTRACT: Photoactive molecules that reversibly switch upon visible light irradiation are one of the most attractive targets for biological as well as imaging applications. One possible approach to prepare such photoswitches is to extend π-conjugation length of molecules and shift the absorption bands to longer wavelengths. Although several attempts have been demonstrated based on this approach for diarylethene (DAE) photoswitches, photoreactivity of the DAE derivatives is dramatically suppressed when the conjugation length is extended by connecting aromatic dyes at the side positions of aryl groups in the DAE unit. In this study, we successfully prepared a visible-light reactive DAE derivative by introducing an aromatic dye at the reactive carbon atom of the DAE unit, optimizing orbital level of each component, and controlling the mutual orientation of the aromatic dye and the DAE unit. The DAE derivative (**3**) undergoes a photocyclization reaction upon irradiation with 560 nm light and the closed-isomer converts to the open-ring isomer upon irradiation with 405 nm light. The high photoconversion yields (>90%) were achieved for both photocyclization and photocycloreversion reactions. The photoreactivity induced by visible light irradiation and the molecular design strategy were discussed based on theoretical calculations.

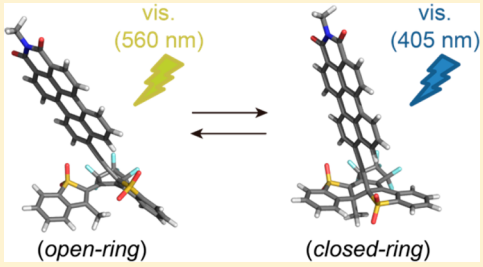

INTRODUCTION

Reversible photoreactions of photochromic molecules have advanced the area of smart materials, and their potential use as key components of molecular electronics, optical memories, and molecular machines has been well documented.[1−6] In particular, microscopic and biological applications of the photoswitches such as super-resolution imaging, biological markers, and bioactivity controls, have recently attracted extensive attention.[7−14] Among a wide variety of photochromic molecules, a family of diarylethene (DAE) derivatives is one of the most attractive molecules because of their excellent thermal stability of both (the open- and the closed-ring) isomers, rapid photoresponse, and high fatigue resistance.[15−18] In the photochromism of most of DAEs, the photocyclization reaction takes place upon irradiation with ultraviolet (UV) light. UV light, however, has drawbacks such as low transparency for commonly used optical components as well as mutagenesis of cells. Therefore, it is desired to develop photochromic molecules, which undergo reversible isomerization reactions upon only visible light irradiation. Such visible light-driven azobenzene-based photoswitches have recently been developed.[19,20]

Among several approaches, such as intramolecular energy transfer via triplet states,[21−24] multiphoton processes,[25] or upconversion luminescence,[26] to achieve visible or NIR-light photoreactivity, the simplest one is to extend π-conjugation length by connecting aromatic dyes which have highly extended π-electron systems and shift the absorption bands in visible or NIR regions. Although several DAE derivatives bearing aromatic dyes at the side positions of the aryl groups were synthesized,[27−29] their photoreactivity was dramatically suppressed since the contribution of the excited singlet state of the central hexatriene part decreases with the extension of π-conjugation.

To overcome the defect, we introduced an aromatic dye into the central reactive carbon atom of the DAE unit. We prepared DAE derivatives possessing a fluorescent perylene di- or monoimide (PDI or PMI) dye at the reactive carbon atom via a π-conjugated spacer and studied their photochromic and fluorescent photoswitching properties.

Received: September 3, 2014
Published: November 12, 2014

dx.doi.org/10.1021/ja5090749 | J. Am. Chem. Soc. 2014, 136, 17145−17154

Scheme 1. Molecular Structures of Compounds 1−6 and Photoswitching of the π-Conjugation Length along with Photocyclization and Photocycloreversion Reactions

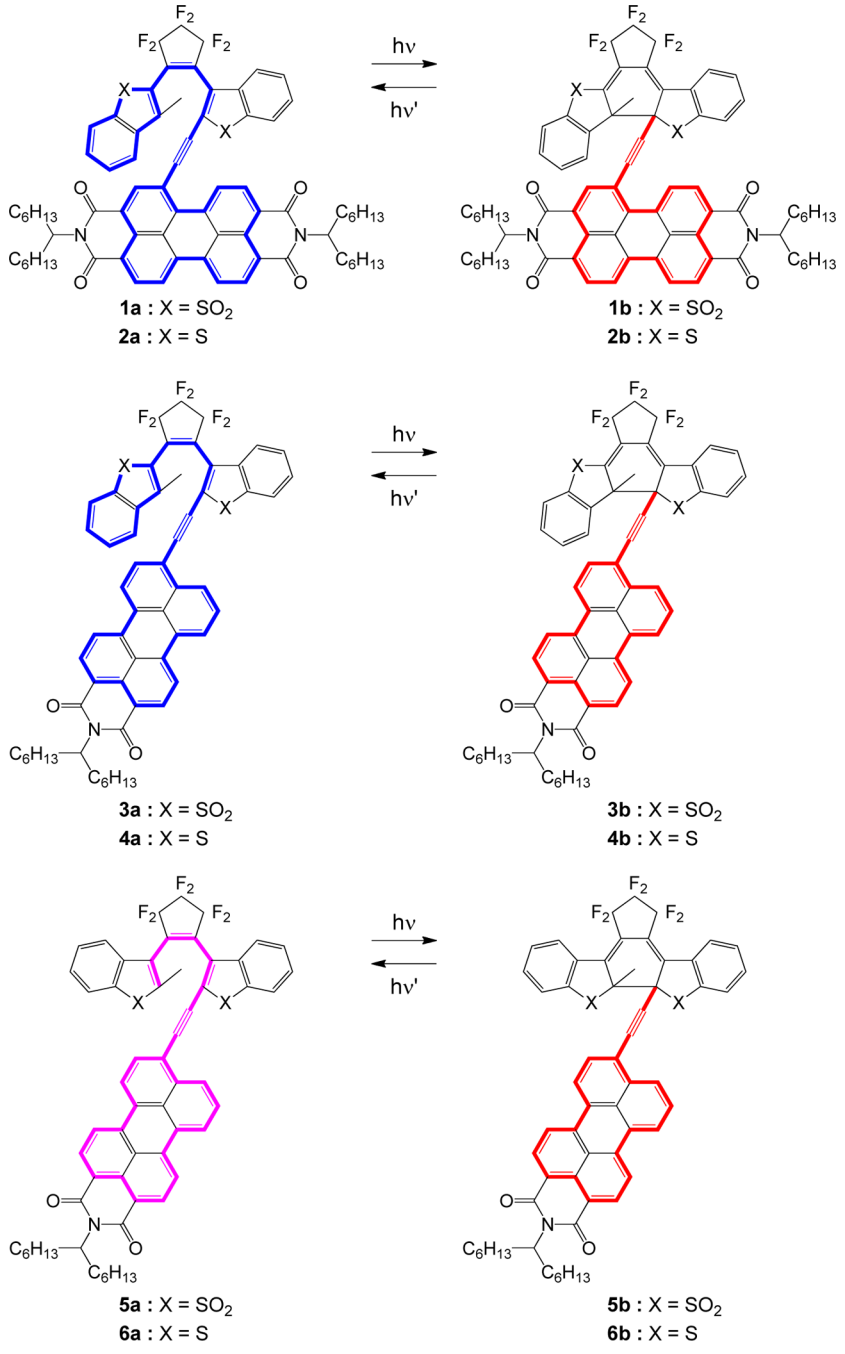

RESULTS AND DISCUSSION

Design, Synthesis, and Structural Characterizations. The compounds we prepared are shown in Scheme 1. These compounds **1**−**6** have a fluorescent *N*,*N*′-bis(1-hexylheptyl)-perylene-3,4:9,10-tetra-carboxylic diimide (PDI) or *N*-bis(1-hexylheptyl)perylene-3,4-dicarboxylic monoimide (PMI) unit at the reactive carbon atom of the DAE unit via a π-conjugated acetylene bond. PDI and PMI derivatives have outstanding stability, excellent photophysical properties such as large molar absorption coefficients, high fluorescence quantum yields, and easiness of synthetic modifications.[30−32] As shown in Scheme 1, the π-conjugation length extends throughout the molecule in the open-ring isomer, while the extended π-conjugation breaks in the closed-ring isomer because the orbital hybridization changes from sp^2 to sp^3 at the reactive carbon atoms of the DAE unit along with the photocyclization reaction.[33−35] In compounds **1**−**4**, one side of aryl (benzothiophene or benzothiophene-1,1-dioxide) groups is connected to the perfluorocyclopentene ring at 2-position, resulting in extension of the π-conjugation length in the open-ring isomer. On the other hand, both aryl groups of the DAE unit are connected to the perfluorocyclopentene ring at 3-position in compounds **5** and **6**. Compounds **7**−**10** (Scheme 2), which have PMI units at the side positions of the DAE unit, were also prepared as references.

dx.doi.org/10.1021/ja5090749 | J. Am. Chem. Soc. 2014, 136, 17145−17154

Scheme 2. Molecular Structures of Reference Compounds 7−10, PDI-acetylene, PMI-acetylene, 2,3′-DAEs, and 3,3′-DAEs

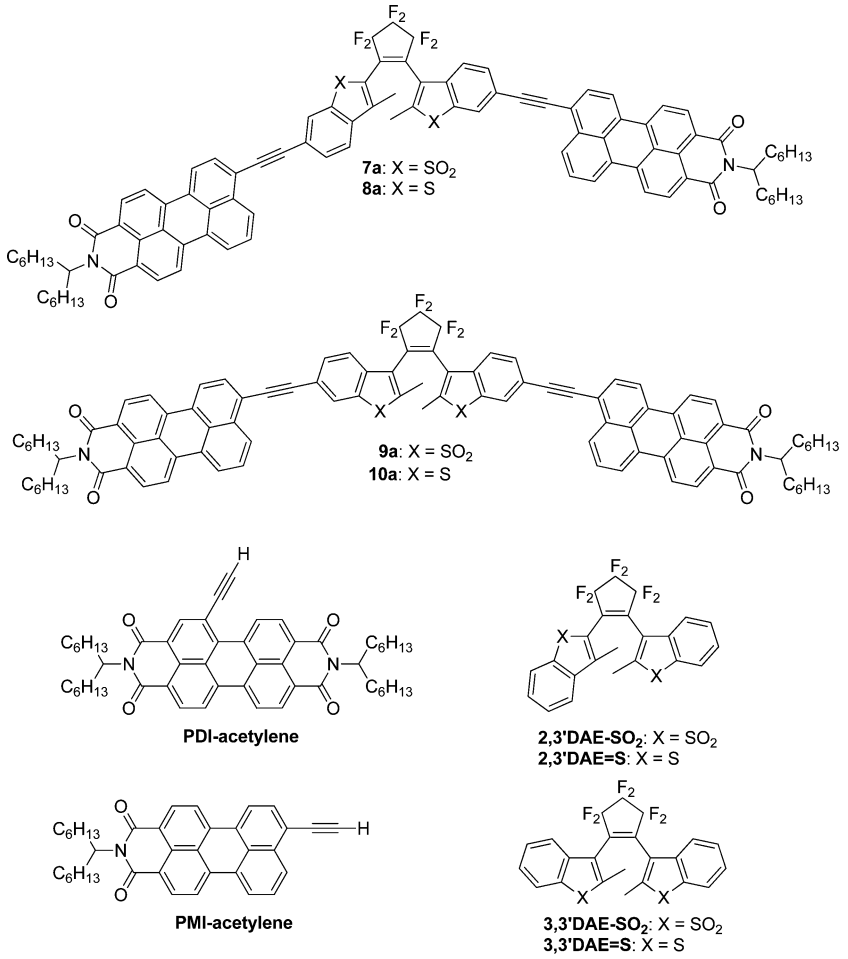

The synthetic routes to compounds **1**−**6** are illustrated in Schemes 3 and 4. Detail synthetic procedures of compounds **7**−**10** were described in Supporting Information. All compounds were structurally characterized by ^{1}H NMR spectroscopy, mass spectrometry, and elemental analysis.

Photoresponsive Properties. Compounds **8**−**10** did not show any spectral change upon irradiation with any wavelength of light from UV to visible regions similarly as reported previously[27] (Figures S8−S10 in Supporting Information). Although compound **7** showed absorption and fluorescence spectral changes upon irradiation with 365 nm light (Supporting Information Figure S7), the spectral change was irreversible and it could not be attributed to the photocyclization reaction of the DAE unit (i.e., photodecomposition). These results indicate that introduction of aromatic dyes at the side positions of aryl groups is not effective to provide visible-light reactivity to DAE.

Figure 1 shows the absorption and fluorescence spectral changes of **1** upon irradiation with 560 nm light in 1,4-dioxane solution. The open-ring isomer **1a** has strong absorption bands at 554 and 412 nm and a broad fluorescence band at around 580 nm. The absorption and fluorescence maxima are longer than that of the terminal acetylene PDI unit (**PDI-acetylene**) (Table 1 and Figure S1 in Supporting Information). The spectra indicate that **1a** has extended π-conjugation to the central hexatriene structure (Supporting Information Figure S12). Upon irradiation with 560 nm light, the absorption band at 554 nm gradually decreases and a spectrum having a characteristic vibrational structure attributable to PDI chromophore appears. Fluorescence spectral change was also observed upon irradiation with 560 nm light, in which the fluorescence band around 580 nm gradually decreases and a new fluorescence band appears around 550 nm. These spectral changes suggest that the π-conjugation length of **1a** becomes short along with the photocyclization reaction. To confirm that these spectral changes are due to the photocyclization reaction of **1a**, ^{1}H NMR and mass spectra of the photoproduct isolated with HPLC were measured. The spectra indicated that the structure of the photoproduct is assigned to the closed-ring isomer (**1b**) (Supporting Information Figure S13). From the absorption spectra of the isolated closed-ring isomer, the conversion from the open- to the closed-ring isomer was revealed to be quantitative. Very unfortunately, the isolated closed-ring isomer was silent upon photoirradiation. Any absorption and fluorescence spectral change was not observed upon irradiation with any wavelength of light.

Figure 2 shows the absorption and fluorescence spectral changes of **3** upon alternate irradiation with 560 and 405 nm light in 1,4-dioxane. The open-ring isomer **3a** has absorption bands at 543 and 350 nm, and exhibits a broad fluorescence band at 550−750 nm. The absorption and fluorescence maxima are longer than those of the terminal acetylene PMI unit (**PMI-acetylene**) (Table 1 and Supporting Information Figure S2), which indicates that the π-conjugation of the PMI unit extends to the central hexatriene structure. In compound **3**, reversible absorption and fluorescence spectral changes were observed

dx.doi.org/10.1021/ja5090749 | J. Am. Chem. Soc. 2014, 136, 17145−17154

Scheme 3. Synthesis of Compounds 1a−4a[a]

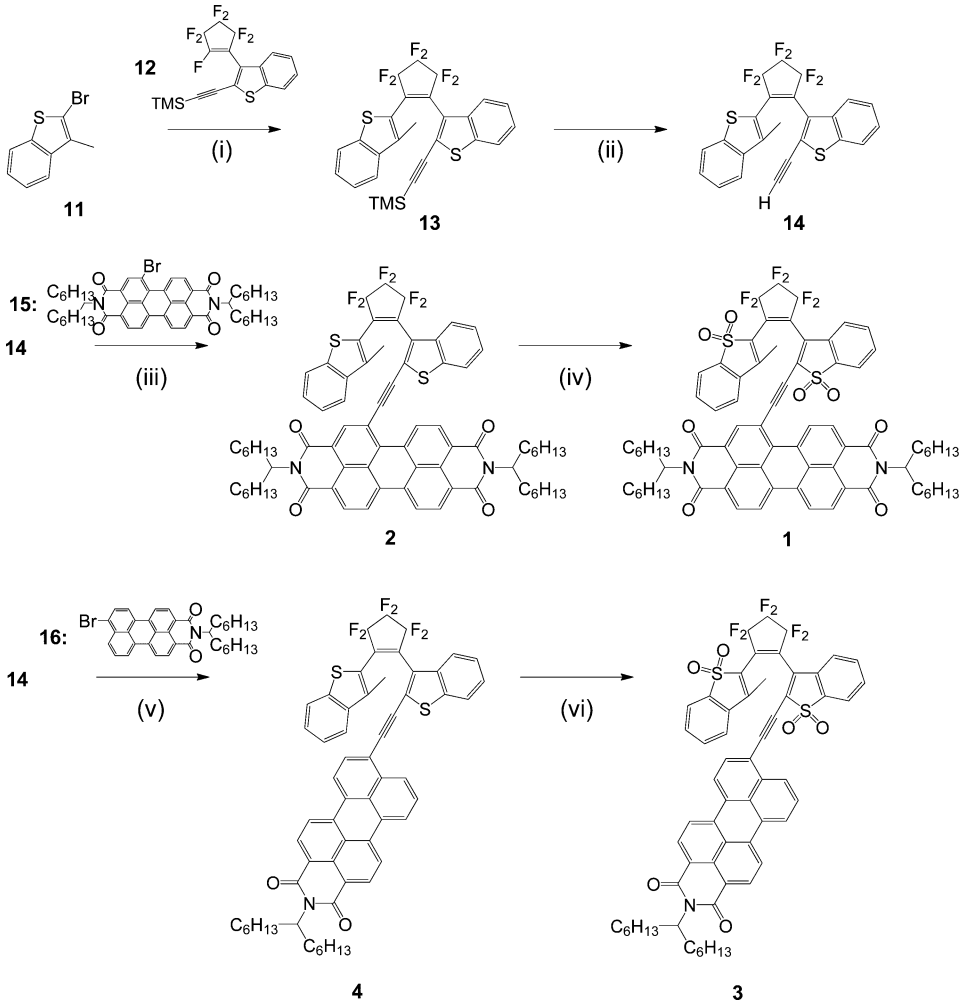

[a](i) *n*-BuLi, **12**, dry THF, −78 °C, 1 h; (ii) TBAF, THF, r.t., 30 min, 43% (over two steps); (iii) **15**, $Pd(PPh_3)_4$, CuI, Et_3N, 75 °C, 20 h, 86%; (iv) *m*CPBA, CH_2Cl_2, r.t., overnight, 77%; (v) **16**, $Pd(PPh_3)_4$, CuI, Et_3N/toluene (1/1), 75 °C, 20 h, 59%; (vi) *m*CPBA, CH_2Cl_2, r.t., overnight, 37%.

upon alternate irradiation with different wavelengths of visible light. Upon irradiation with 560 nm light the absorption band at 543 nm gradually decreases with increasing absorption bands around 500 and 350 nm (Figure 2a). Upon irradiation with 405 nm light, these absorption bands turn back to the initial one. The spectral changes are attributed to photocyclization and photocycloreversion reactions of compound **3** (Supporting Information Figure S14). The absorption spectrum of **3b** isolated with HPLC indicates that the conversion ratio from the open- to the closed-ring isomer at the photostationary state (PSS) under irradiating with 560 nm is 97% and the ratio from the closed- to the open-ring isomer at the PSS under irradiating with 405 nm light is 90%. The high photoconversion ratio under irradiating with 560 nm light is attributed to the excitation wavelength dependence of the photocycloreversion quantum yield of **3b**. The photocycloreversion reaction of **3b** exhibited excitation wavelength dependence, as shown in Supporting Information Figure S11. The quantum yield decreases to almost zero upon excitation with >450 nm light. The wavelength dependence of **3b** suggests that the π-conjugation completely breaks in the closed-ring isomer and each component absorbs photons independently. The DAE unit has no absorbance at the wavelength region longer than 450 nm (Supporting Information Figure S12). The absorption band longer than 450 nm is attributed to the isolated PMI unit. Photoexcitation of the PMI unit cannot induce the cycloreversion reaction. Therefore, 560 nm light provides the high photoconversion yield from the open- to the closed-ring isomer.

The broad fluorescence band at 550−750 nm region decreases along with the increase in the fluorescence band at 540 nm upon irradiation with 560 nm light, as shown in Figure 2b. The 540 nm fluorescence band returns to the original 550−750 nm band upon irradiation with 405 nm light. Fluorescence quantum yield of **3a** (Φ_f = 0.016) was significantly decreased in comparison with that of **PMI-acetylene** (Φ_f = 0.94). The absorption and fluorescence maxima of the closed-ring isomer are almost similar to that of **PMI-acteylene** (Table 1), which indicates the π-conjugation length becomes short upon the photocyclization reaction. The absorption and fluorescence spectral changes can be repeated for many cycles (at least over 10 cycles) without notable spectral changes. In addition, the photogenerated isomer **3b** is thermally stable similar to typical DAE derivatives, where no spectral change is observed even after 7 days in the dark condition at 25 °C. Absorption maxima, absorption coefficients, fluorescence maxima, photoconversion ratios, fluorescence quantum yields, and the quantum yield of photoreactions of compounds **1** and **3** are summarized in Table

dx.doi.org/10.1021/ja5090749 | J. Am. Chem. Soc. 2014, 136, 17145−17154

Scheme 4. Synthesis of Compounds 5a and 6a[a]

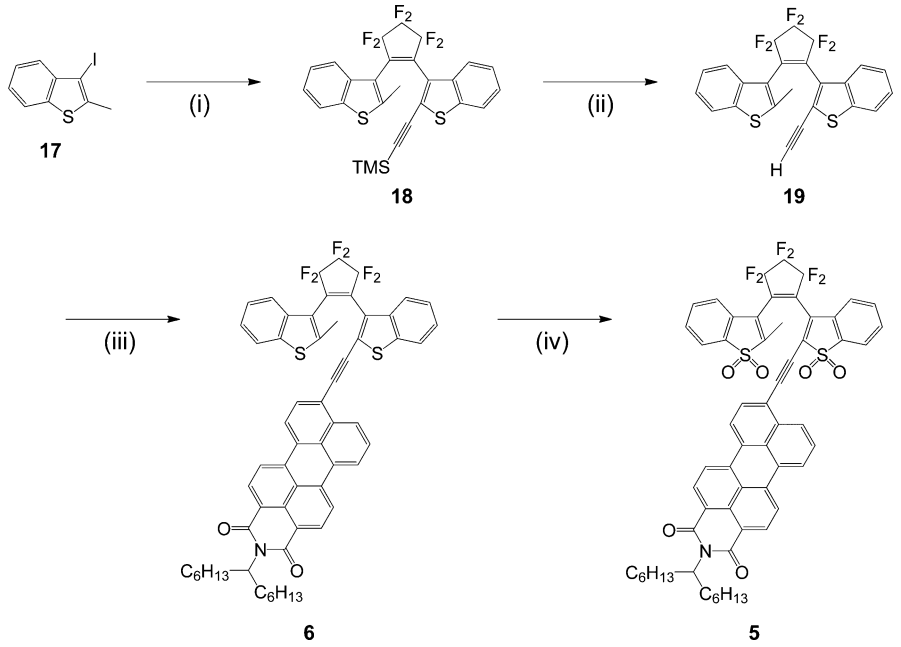

[a](i) *n*-BuLi, **12**, dry THF, −78 °C, 1 h; (ii) TBAF, THF, r.t., 30 min, 61% (over two steps); (iii) **16**, $Pd(PPh_3)_4$, CuI, Et_3N/THF (2/1), 65 °C, 20 h, 73%; (iv) *m*CPBA, CH_2Cl_2, r.t., overnight, 48%.

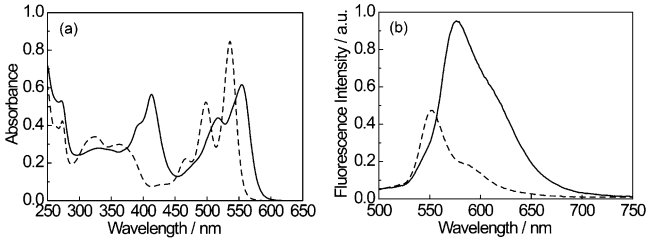

Figure 1. (a) Absorption and (b) fluorescence (uncorrected) spectral changes of **1** in 1,4-dioxane solution along with 560 nm light; the open-ring isomer (**1a**) (solid-line), the closed-ring isomer (**1b**) (dashed-line).

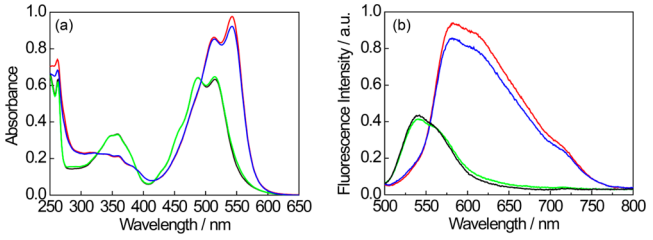

Figure 2. (a) Absorption and (b) fluorescence (uncorrected) spectral changes of **3** in 1,4-dioxane solution upon irradiation with 560 nm (for cyclization) and 405 nm (for cycloreversion) lights; the open- (**3a**) (red), the closed-ring (**3b**) (black), PSS at 560 nm (green), and PSS at 405 nm (blue).

1. In contrast to compounds **1** and **3**, no photoreaction was observed for compounds **2** and **4**−**6** upon irradiation with any wavelength of lights (Supporting Information Figures S3−S6).

Theoretical Calculations. To reveal the difference in photoreactivity between these molecules, theoretical calculations were carried out at the RTD-B3LYP/6-311(2d,p)//RB3LYP/6-31g(d) level of theory.

Molecular orbital correlation diagrams are shown in Figure 3 and Supporting Information Figures S15−S22. The orbital energies of LUMOs of **2,3′-DAE-S**, **2,3′-DAE-SO$_2$**, **3,3′-DAE-**

Table 1. Reaction Quantum Yields of Photocyclization and Photocycloreversion, Absorption and Fluorescence Maxima, Photoconversion Ratios and Fluorescence Quantum Yields of 1a, 1b, 3a, 3b, PDI-acetylene, and PMI-acetylene in 1,4-Dioxane Solution

compound	1a	1b	PDI-acetylene	3a	3b	PMI-acetylene
Φ (O → C)	3.1×10^{-3}[a]	-	-	6.4×10^{-4}[a]	-	-
Φ (C → O)	-	0[b]	-	-	5.2×10^{-3}[c],0[d]	-
λ_{max} (abs)	554 nm	536 nm	527 nm	543 nm	515 nm	510 nm
(ε/$M^{-1}cm^{-1}$)	(46,400)	(63,700)	(81,200)	(43,900)	(28,200)	(28,300)
λ_{em}	575 nm	552 nm	543 nm	568 nm	540 nm	534 nm
Conversion/%	>99	0	-	97	90	-
($\lambda_{irrad.}$)	(560 nm)	(405 nm)	-	(560 nm)	(405 nm)	-
Φ_f[e]	0.11	0.02	0.92	0.016	0.008	0.94

[a]Measured with 554 nm light. [b]Measured with 405 nm light. [c]Measured with 405 nm light. [d]Measured with 560 nm light. [e]*N*,*N*-bis(1-hexylheptyl)perylene-3,4:9,10-tetracarboxylbisimide (Φ_f = 0.99 in dichloromethane) is used as the reference.

dx.doi.org/10.1021/ja5090749 | J. Am. Chem. Soc. 2014, 136, 17145−17154

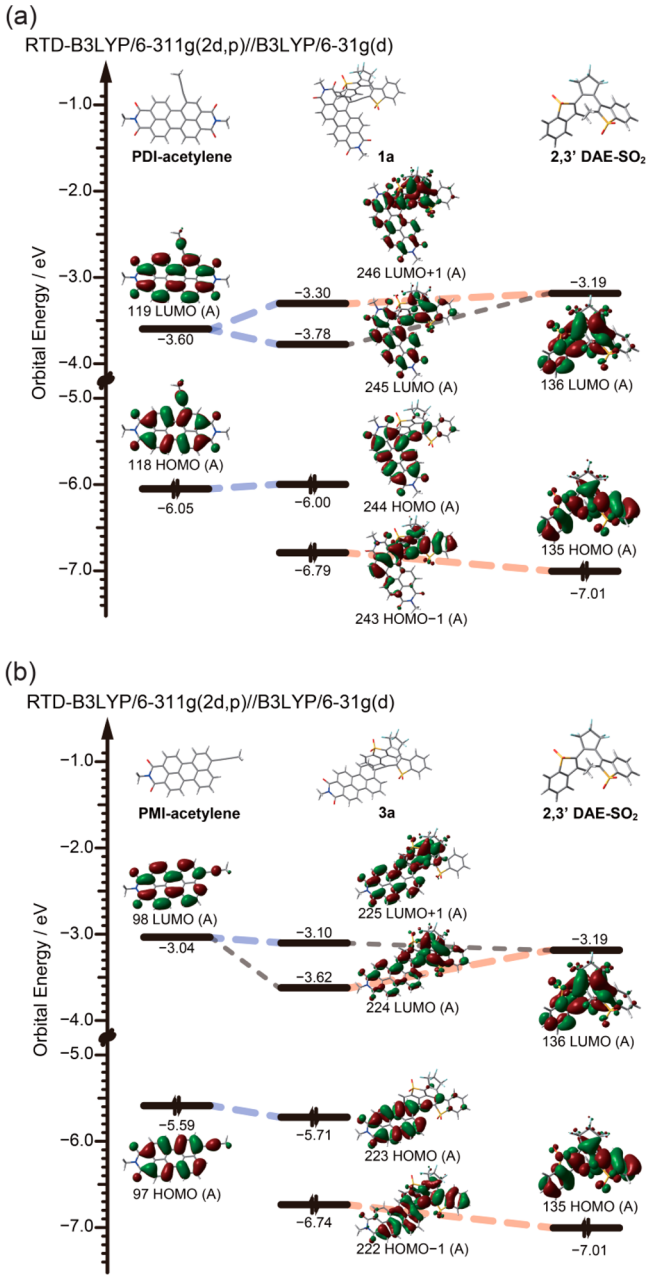

Figure 3. Orbital correlation diagrams of (a) **1a** and (b) **3a** calculated at B3LYP/6-311g(2d,p)//6-31g(d) level of theory.

S, and **3,3′-DAE-SO$_2$** are strongly influenced by (i) the oxidation state of the sulfur atoms and (ii) the substitution position of the benzothiophenyl groups. As summarized in Table 2, HOMO and LUMO energy levels decrease by ∼0.9 eV when the sulfur atoms of benzothiophenyl groups are oxidized. In addition, LUMO energies decrease by ∼0.4 eV when the substitution position of the benzothiophene is changed from 3- to 2-position. Consequently, the LUMO energy of **2,3′-DAE-SO$_2$** is close to those of **PDI-acetylene** or **PMI-acetylene**, resulting in significant orbital interaction between DAE and fluorescent units in the LUMO levels.

As shown in Figure 3, HOMOs of **1a** and **3a** localize in the fluorescent unit (i.e., PDI or PMI unit), while LUMOs of **1a** and **3a** delocalize throughout the molecule (The enlarged figures of LUMOs of **1a**−**6a** are shown in Figure 4). The LUMO characters of compounds **1a** and **3a** are suitable for the photocyclization reaction.[36] On the other hand, as shown in Figure 4 and Supporting Information Figures S15−18, in the case of the other compounds (i.e., **2a**, **4a**, **5a**, and **6a**), LUMOs localize on the PMI unit and do not extend to the hexatriene part. Therefore, the cyclization reactions cannot take place upon photoirradiation of these compounds. The absence of photoreactivity of compounds **7a**−**10a** can also be explained by the localization of LUMO energy to PMI units (Supporting Information Figures S19−22).

Contribution of Intramolecular Energy Transfer. No photoreactivity of **1b** is attributed to the energy transfer from the closed-ring DAE unit to the PDI unit. The absorption band of PDI unit locates at longer wavelengths than that of the closed-ring DAE unit (Supporting Information Figure S12) and the transition dipole moments of both units are oriented almost parallel (Figure 5a). These conditions are suitable for efficient intramolecular energy transfer and therefore the photocycloreversion reaction of **1b** is prohibited. On the other hand, in the case of **3b**, the transition dipole moment of fluorescence unit is perpendicularly oriented to that of the DAE unit (Figure 5b). Such perpendicular orientation is not favorable for the energy transfer, and therefore, it is anticipated that the photocycloreversion reaction can proceed.

To confirm this interpretation, fluorescence excitation spectra of **1b** and **3b** were measured, as shown in Figure 5. In the excitation spectrum of **1b**, a clear excitation band is observed in the region of 300−400 nm, where the closed-ring isomer of DAE unit has absorption band (Figure 5c). This spectrum clearly indicates that both PDI and DAE units contribute to the fluorescence of **1b** and efficient intramolecular energy transfer from the DAE unit to the PDI unit takes place in **1b**. On the other hand, any specific band corresponding to the closed-ring isomer of DAE unit is not observed in the excitation spectrum of **3b**, as shown in Figure 5d. The intramolecular energy transfer is suppressed due to perpendicular orientation of the fluorescent and DAE units. This mechanism can account for the reversible photoreactivity of compound **3**.

■ CONCLUSION

Recently, photochromic study is expanding its application field to biology. For such applications, photoreactivity by irradiation with longer wavelengths of light (i.e., visible or NIR) is indispensable. In this study, we designed and synthesized a DAE derivative that switches upon only visible light irradiation. By (i) introducing an aromatic dye, PDI or PMI, into the reactive carbon atom of the DAE unit, (ii) oxidizing sulfur

Table 2. HOMO and LUMO Energies of Fragments Calculated by the B3LYP/6-311g(2d,p) level

	2,3′-derivatives		3,3′-derivatives			
	DAE-S	DAE-SO$_2$	DAE-S	DAE-SO$_2$	PDI-acetylene	PMI-acetylene
LUMO energy/eV	−2.21	−3.19	−1.87	−2.67	−3.60	−3.04
HOMO energy/eV	−6.16	−7.01	−6.18	−7.18	−6.05	−5.59

dx.doi.org/10.1021/ja5090749 | J. Am. Chem. Soc. 2014, 136, 17145−17154

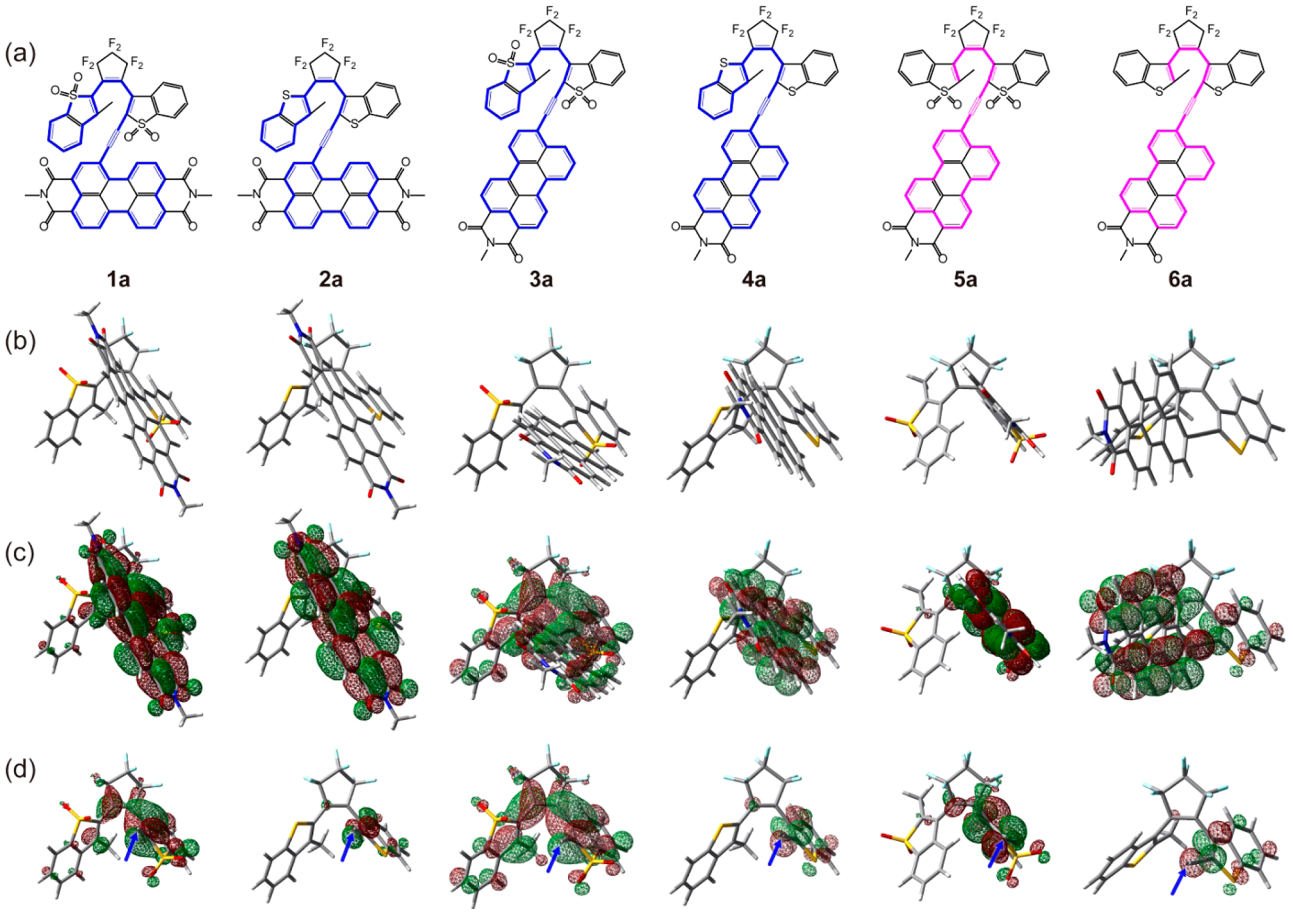

Figure 4. Enlarged view of LUMOs of **1a**–**6a**: (a) the calculated molecular structures, (b) the optimized structures at B3LYP/6-31g(d) level, (c) LUMOs calculated at B3LYP/6-311g(2d,p) level, and (d) enlarged view around the hexatriene part of the diarylethene moiety, in which PDI or PMI moiety was omitted for clarity. Blue arrows represent the position where PDI or PMI moiety is connected.

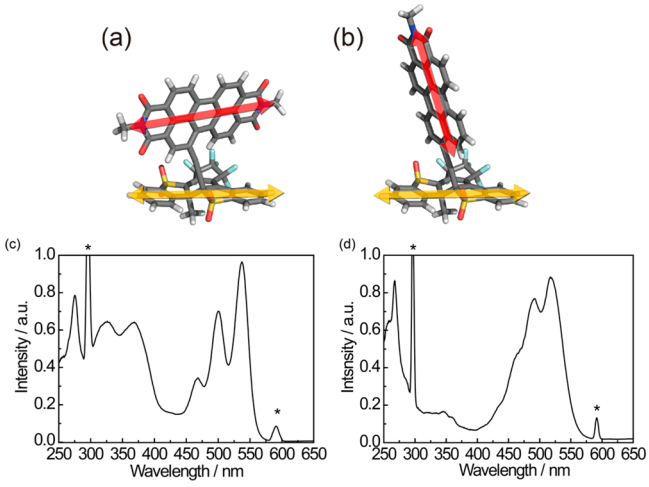

Figure 5. (a and b) Molecular structures of **1b** (a) and **3b** (b) optimized at B3LYP/6-31g(d) level. The arrows indicate the transition dipole moment vectors of fluorescent (red arrow) and DAE (yellow arrow) units for **1b** and **3b**, respectively. (c and d) Excitation spectra of **1b** (c) and **3b** (d) monitored at 590 nm. Peaks marked as "*" are due to the monitor light (590 nm).

atoms of the benzothiophene groups, and (iii) controlling the mutual orientation of the aromatic dye and the DAE unit, we successfully prepared a visible light-driven DAE photoswitch. Our molecular design strategy is promising to prepare advanced DAE derivatives having further longer wavelength (i.e., NIR) light responsiveness.

EXPERIMENTAL SECTION

Materials and Methods. General chemicals were purchased from Tokyo Chemical Industries, Wako Pure Chemicals, or Sigma-Aldrich, and used without further purification. Solvents used in photochemical measurements were of spectroscopic grade and were purified by distillation before use. 1-(3-Bromobenzo[*b*]thiophen-2-yl)-2-trimethylsilylacetylene,[37] 1-bromo-*N*,*N*′-bis(1-hexylheptyl)perylene-3,4:9,10-tetra-carboxylic diimide (**15**)[38] and 9-bromo-*N*-bis(1-hexylheptyl)perylene-3,4-dicarboxylic monoimide (**16**)[39] were prepared according to literature procedures. ^{1}H NMR spectra were recorded on a NMR spectrometer (JEOL, ECX-400, 400 MHz). Samples were dissolved in $CDCl_3$ with tetramethylsilane as an internal standard. Mass spectra were measured with a mass spectrometer (Shimadzu GCMS-QP5050A and Applied-Biosystems Voyger). Absorption and fluorescence spectra were measured with a Hitachi U-3310 absorption spectrophotometer and a Hitachi F-2500 fluorescence spectrophotometer, respectively. Fluorescence quantum yields were determined by using a monochromatic 500 nm as the excitation light source, a very dilute solution, the absorbance of which is less than 0.02 at the excitation wavelength for all solvents, and *N*,*N*′-bis(1-hexylheptyl)perylene-3,4:9,10-tetracarboxylbisimide (Φ_f = 0.99, in dichloromethane) as the reference.[40] Photoirradiation was carried out using a xenon lamp (MAX-303, Asahi Spectra) as the light source. Monochromic light was obtained by passing the light through a monochromator (Jobin-Yvon) or a band-pass filter ($\Delta\lambda_{1/2}$ = 15 nm). The geometrical optimization was carried out at the RB3LYP/6-31g(d) level of theory implemented on Gaussian 09 package.[41] Long

dx.doi.org/10.1021/ja5090749 | J. Am. Chem. Soc. 2014, 136, 17145–17154

alkyl chains of the fluorescent unit (PDI or PMI) in **1a−10a** were replaced by methyl groups to simplify the system. To model the geometry of fragments of **1a−10a** (i.e., **2,3′-DAE-SO$_2$**, **2,3′-DAE-S**, **3,3′-DAE-SO$_2$**, **3,3′-DAE-S**, **PDI-acetylene** and **PMI-acetylene**), the ends of fragments were also replaced by methyl groups. Convergence at a local minimum structure was confirmed by no imaginary frequencies on frequency analysis. Successively, the optimized local minimum structures were subjected to time-dependent (TD) DFT calculations in the gas phase to obtain 10 excited states from the lowest energy transitions at the RB3LYP/6-311g(2d,p) level of theory.

*Compound **14**.* Under argon atmosphere, *n*-butyllithium hexane solution (3.3 mL, 5.4 mmol) was slowly added to the solution of 1-(3-bromobenzo[*b*]thiophen-2-yl)-2-trimethylsilylacetylene (1.5 g, 4.9 mmol) in dry THF (45 mL) at −78 °C. After 30 min, octafluorocyclopentene (1.4 mL, 10.4 mmol) was added to the reaction mixture at −78 °C. The mixture was left to reach room temperature. After 1.5 h, the reaction was stopped by the addition of water. The product was extracted with diethyl ether and washed with brine three times. The organic layer was dried over $MgSO_4$, filtered, and concentrated. The residue was purified by using silica gel column chromatography with hexane as the eluent. Compound **12** was obtained as a white solid (1.54 g 75%).

^{1}H NMR (400 MHz $CDCl_3$) δ 0.26 (s, 9H), 7.42−7.50 (m, 2H), 7.64−7.70 (m, 1H), 7.78−7.83 (m, 1H); MS m/z = 422 $[M]^+$. Anal. Calcd for $C_{18}H_{13}F_7S$: C, 51.18; H, 3.10. Found: C, 51.16; H, 3.07.

Under argon atmosphere, *n*-butyllithium hexane solution (740 μL, 1.2 mmol) was slowly added to the solution of **11** (245 mg, 1.1 mmol) in dry THF (10 mL) at −78 °C. After the mixture was stirred for 1 h, **12** (500 mg, 1.2 mmol) in dry THF (5 mL) was slowly added and the solution was stirred for 30 min at −78 °C. When the reaction mixture cooled to room temperature, it was extracted by ether, dried over anhydrous magnesium sulfate, and concentrated. The crude product **13** was dissolved to dry THF (20 mL) and stirred for 5 min. A 1.0 M tetrabutylammonium fluoride solution in THF (1.5 mL, 1.5 mmol) was slowly added to the mixture solution and then stirred for 30 min. The reaction mixture was extracted with ether, dried over anhydrous magnesium sulfate, and concentrated. The residue was purified by silica gel column chromatography (hexane/ethyl acetate = 95/5) to give 220 mg (0.46 μmol) of **14** in 43% yield (over two steps) as yellow solid.

^{1}H NMR (400 MHz $CDCl_3$) δ 2.09 (s, 3H), 3.60 (s, 1H), 7.30−7.37 (m, 2H), 7.38−7.44 (m, 2H), 7.55−7.61 (m, 1H), 7.63−7.68 (m, 1H), 7.70−7.76 (m, 2H); MS m/z = 478 $[M]^+$. Anal. Calcd for $C_{24}H_{12}F_6S_2$: C, 60.25; H, 2.53. Found: C, 60.27; H, 2.51.

*Compound **2**.* The solution of **14** (50 mg, 104 μmol) and 1-bromo-*N*,*N*′-bis(1-hexylheptyl)perylene- 3,4:9,10-tetracarboxylic diimide (100 mg, 120 μmol), CuI (2.5 mg, 13 μmol) and $Pd(PPh_3)_4$ (14 mg, 12 μmol) in triethylamine (3 mL) was purged with argon gas for 20 min and then refluxed at 75 °C for 20 h. After being cooled, the triethylamine (Et_3N) was evaporated. The residue was extracted with $CHCl_3$, dried over anhydrous magnesium sulfate, and concentrated. The residue was purified by silica gel column chromatography ($CHCl_3$/hexane =6/4) to give 110 mg (90 μmol) of **2** in 86% yield as dark red solid.

^{1}H NMR (400 MHz, $CDCl_3$) δ 0.80−0.87 (m, 12H), 1.20−1.42 (m, 32H), 1.82−1.93 (m, 4H), 2.05 (s, 3H), 2.19−2.32 (m, 4H), 5.15−5.23 (m, 2H), 7.13−7.25 (m, 2H), 7.44−7.56 (m, 4H), 7.80 (d, J = 7.6 Hz, 1H), 7.84−7.89 (m, 1H), 8.44 (brs, 1H), 8.62−8.80 (m, 5H), 9.70 (d, J = 8 Hz, 1H); FAB-MS m/z = 1231 $[M + 1]^+$. Anal. Calcd for $C_{74}H_{72}F_6N_2O_4S_2$: C, 72.17; H, 5.89; N, 2.27. Found: C, 72.08; H, 5.92; N, 2.25.

*Compound **1**.* The solution of **2** (48 mg, 39 μmol) and 65% *m*-chloroperoxybenzoic acid (mCPBA) (62 mg, 234 μmol) in CH_2Cl_2 (3 mL) was stirred overnight at room temperature. After then, $NaHCO_3$ solution was added to the reaction mixture and extracted by dichloromethane, dried over anhydrous magnesium sulfate, and concentrated. The residue was purified by silica gel column chromatography ($CHCl_3$) to give 39 mg (30 μmol) of **1** in 77% yield as dark red solid.

1a: ^{1}H NMR (400 MHz, $CDCl_3$) δ 0.80−0.87 (m, 12H), 1.17−1.42 (m, 32H), 1.82−1.94 (m, 4H), 2.19−2.30 (m, 4H), 2.33 (s, 3H), 5.14−5.24 (m, 2H), 7.37−7.44 (m, 1H), 7.51−7.60 (m, 3H), 7.63−7.72 (m, 3H), 7.82−7.85 (m, 1H), 8.69−8.86 (m, 6H), 10.09 (d, J = 7.6 Hz, 1H); FAB-MS m/z = 1295 $[M + 1]^+$. Anal. Calcd for $C_{74}H_{72}F_6N_2O_8S_2$: C, 68.61; H, 5.60; N, 2.16. Found: C, 68.66; H, 5.58; N, 2.17.

1b: ^{1}H NMR (400 MHz $CDCl_3$) δ 0.79−0.89 (m, 12H), 1.12−1.41 (m, 32H), 1.78−1.91 (m, 4H), 2.04 (s, 3H), 2.18−2.35 (m, 4H), 5.06−5.23 (m, 2H), 7.62−7.71 (m, 1H), 7.87−8.07 (m, 5H), 8.16−8.26 (m, 2H), 8.33 (d, J = 8.0 Hz, 1H), 8.45 (d, J = 8.0 Hz, 1H), 8.54−8.71 (m, 4H), 9.20−9.33 (m, 1H); MS (MALDI) m/z = 1294 $[M]^+$.

*Compound **4**.* The mixture solution of **14** (55 mg, 115 μmol) and 9-bromo-*N*-bis(1-hexylheptyl)perylene-3,4-carboxylic monoimide (76 mg, 130 μmol), CuI (2.0 mg, 10 μmol) and $Pd(PPh_3)_4$ (14 mg, 12 μmol) in triethylamine (Et_3N)/toluene (1/1) (4.0 mL) was purged with argon gas for 20 min and then stirred at 75 °C for 20 h. After being cooled, the triethylamine was evaporated. The residue was extracted with $CHCl_3$, dried over anhydrous magnesium sulfate, and concentrated. The residue was purified by silica gel column chromatography ($CHCl_3$/hexane =6/4) to give 75 mg (77 μmol) of **4** in 59% yield as dark red solid.

^{1}H NMR (400 MHz $CDCl_3$) δ 0.80−0.87 (m, 6H), 1.20−1.42 (m, 16H), 1.82−1.95 (m, 2H), 2.11 (s, 3H), 2.20−2.33 (m, 2H), 5.17−5.26 (m, 1H), 7.27−7.32 (m, 2H), 7.42−7.49 (m, 2H), 7.51−7.57 (m, 1H), 7.58−7.67 (m, 2H), 7.72−7.85 (m, 3H), 8.22−8.39 (m, 5H), 8.47−8.61 (m, 2H); FAB-MS m/z = 980 $[M+1]^+$. Anal. Calcd for $C_{59}H_{47}F_6NO_2S_2$: C, 72.30; H, 4.83; N, 1.43. Found: C, 72.27; H, 4.88; N, 1.48.

*Compound **3**.* The solution of **4** (48 mg, 39 μmol) and 65% mCPBA (53 mg, 200 μmol) in CH_2Cl_2 (1.5 mL) was stirred overnight at room temperature. After then, $NaHCO_3$ solution was added to the reaction mixture and extracted by dichloromethane, dried over anhydrous magnesium sulfate, and concentrated. The residue was purified by silica gel column chromatography ($CHCl_3$) to give 12 mg (11.5 μmol) of **1** in 37% yield as dark red solid.

3a: ^{1}H NMR (400 MHz $CDCl_3$) δ 0.78−0.90 (m, 6H), 1.13−1.43 (m, 16H), 1.80−1.93 (m, 2H), 2.18−2.32 (m, 5H), 5.15−5.25 (m, 1H), 7.38−7.42 (m, 1H), 7.50−7.54 (m, 1H), 7.55−7.72 (m, 5H), 7.76−7.83 (m, 2H), 7.94 (d, J = 8.0 Hz, 1H), 8.36 (d, J = 8.0 Hz, 1H), 8.44 (d, J = 8.0 Hz, 1H), 8.46−8.52 (m, 2H), 8.54 (d, J = 8.0 Hz, 1H), 8.58−8.68 (m, 2H); MS (MALDI) m/z = 1044 $[M + 1]^+$. Anal. Calcd for $C_{59}H_{47}F_6NO_6S_2$: C, 67.87; H, 4.54; N, 1.34. Found: C, 67.92; H, 4.58; N, 1.39.

3b: ^{1}H NMR (400 MHz $CDCl_3$) δ 0.78−0.88 (m, 6H), 1.14−1.34 (m, 16H), 1.78−1.86 (m, 2H), 2.01 (s, 3H), 2.17−2.26 (m, 2H), 5.13−5.19 (m, 1H), 7.39 (d, J = 8.0 Hz, 1H), 7.49 (t, J = 8.0 Hz, 1H), 7.60 (d, J = 8.0 Hz, 1H), 7.67 (t, J = 8.0 Hz, 1H), 7.85−8.01 (m, 4H), 8.09 (d, J = 8.0 Hz, 1H), 8.13−8.18 (m, 1H), 8.20−8.35 (m, 4H), 8.39−8.44 (m, 1H), 8.46−8.56 (m, 2H); MS (MALDI) m/z = 1044 $[M+1]^+$.

*Compound **19**.* Under argon atmosphere, *n*-butyllithium hexane solution (1.5 mL, 2.5 mmol) was slowly added to the solution of **17** (600 mg, 2.2 mmol) in dry THF (20 mL) at −78 °C. After the mixture was stirred for 1 h, **12** (1.0 g, 2.4 mmol) in dry THF (10 mL) was slowly added and the solution was stirred for 30 min at −78 °C. When the reaction mixture cooled to room temperature, it was extracted by ether, dried over anhydrous magnesium sulfate, and concentrated. The crude product **18** was dissolved to dry THF (50 mL) and stirred for 5 min. A 1.0 M tetrabutylammonium fluoride solution in THF (3.0 mL, 3.0 mmol) was slowly added to the mixture solution and then stirred for 30 min. The reaction mixture was extracted with ether, dried over anhydrous magnesium sulfate, and concentrated. The residue was purified by silica gel column chromatography (hexane/ethyl acetate = 98/2) to give 640 mg (1.3 mmol) of **19** in 61% yield (over two steps) as yellow solid.

^{1}H NMR (400 MHz $CDCl_3$) δ 2.25, 2.52 (2s, 3H), 3.37, 3.57 (2s, 1H), 7.18−7.75 (m, 8H); MS m/z = 478 $[M]^+$. Anal. Calcd for $C_{24}H_{12}F_6S_2$: C, 60.25; H, 2.53. Found: C, 60.33; H, 2.56.

dx.doi.org/10.1021/ja5090749 | J. Am. Chem. Soc. 2014, 136, 17145−17154

Compound **6**. The mixture solution of **19** (150 mg, 314 μmol) and **16** (300 mg, 515 μmol), CuI (6.0 mg, 50 μmol) and $Pd(PPh_3)_4$ (20 mg, 17 μmol) in Et_3N/THF (2/1) (3.0 mL) was purged with argon gas for 20 min and then stirred at 65 °C for 20 h. After being cooled, the solvent was evaporated. The residue was extracted with $CHCl_3$, dried over anhydrous magnesium sulfate, and concentrated. The residue was purified by silica gel column chromatography ($CHCl_3$/MeOH = 95/5) to give 224 mg (229 μmol) of **6** in 73% yield as dark red solid.

^{1}H NMR (400 MHz $CDCl_3$) δ 0.77−0.88 (m, 6H), 1.13−1.47 (m, 16H), 1.78−1.96 (m, 2H), 2.13−2.55 (m, 5H), 5.13−5.27 (m, 1H), 7.28−7.97 (m, 10H), 8.25−8.73 (m, 7H); MS (MALDI) m/z = 981 $[M+1]^+$. Anal. Calcd for $C_{59}H_{47}F_6NO_2S_2$: C, 72.30; H, 4.83; N, 1.43. Found: C, 72.25; H, 4.84; N, 1.44.

Compound **5**. The solution of **6** (100 mg, 102 μmol) and 65% mCPBA (160 mg, 650 μmol) in CH_2Cl_2 (4.0 mL) was stirred overnight at room temperature. After then, $NaHCO_3$ solution was added to the reaction mixture and extracted by dichloromethane, dried over anhydrous magnesium sulfate, and concentrated. The residue was purified by silica gel column chromatography ($CHCl_3$/MeOH = 95/5) to give 51 mg (49 μmol) of **5** in 48% yield as dark red solid.

^{1}H NMR (400 MHz $CDCl_3$) δ 0.76−0.87 (m, 6H), 1.15−1.39 (m, 16H), 1.79−1.91 (m, 2H), 2.14 (s, 3H), 2.19−2.30 (m, 2H), 5.13−5.27 (m, 1H), 7.15−7.95 (m, 10H), 8.16−8.71 (m, 7H); MS (MALDI) m/z = 1045 $[M + 1]^+$. Anal. Calcd for $C_{59}H_{47}F_6NO_6S_2$: C, 67.87; H, 4.54; N, 1.34. Found: C, 67.89; H, 4.48 N, 1.35.

■ ASSOCIATED CONTENT

Ⓢ Supporting Information

Detailed synthetic procedures, absorption and fluorescence spectra, and the supporting data of theoretical calculations. This material is available free of charge via the Internet at http://pubs.acs.org.

■ AUTHOR INFORMATION

Corresponding Authors

tuyoshi@es.hokudai.ac.jp

iriem@rikkyo.ac.jp

Notes

The authors declare no competing financial interest.

■ ACKNOWLEDGMENTS

This work was supported by PRESTO ("Innovative Use of Light and Materials/Life" area), Japan Science and Technology Agency (JST) and a Grant-in-Aid for Young Scientist (A) (No. 24685201). We thank to Prof. M. Morimoto for kindly measuring some undescribed data.

■ REFERENCES

(1) Feringa, B. L. *J. Org. Chem.* **2007**, *72*, 6635−6652.

(2) Kawata, S.; Kawata, Y. *Chem. Rev.* **2000**, *100*, 1777−1788.

(3) Willner, I.; Willner, B. *Pure Appl. Chem.* **2001**, *73*, 535−542.

(4) Bouas-Laurent, H.; Dürr, H. *Pure Appl. Chem.* **2001**, *73*, 639−665.

(5) Irie, M. *Bull. Chem. Soc. Jpn.* **2008**, *81*, 917−926.

(6) Bianco, A.; Perissinotto, S.; Garbugli, M.; Lanzani, G.; Bertarelli, C. *Laser Photonics Rev.* **2011**, *5*, 711−736.

(7) Hell, S. W. *Science* **2007**, *316*, 1153−1158.

(8) Heilemann, M.; Dedecker, P.; Hofkens, J.; Sauer, M. *Laser Photonics Rev.* **2009**, *3*, 180−202.

(9) Fukaminato, T. *J. Photochem. Photobiol. C* **2011**, *12*, 177−208.

(10) Mayer, G.; Heckel, A. *Angew. Chem., Int. Ed.* **2006**, *45*, 4900−4921.

(11) Fehrentz, T.; Schönberger, M.; Trauner, D. *Angew. Chem., Int. Ed.* **2011**, *50*, 12156−12182.

(12) Beharry, A. A.; Woolley, G. A. *Chem. Soc. Rev.* **2011**, *40*, 4422−4437.

(13) Brieke, C.; Rohrbach, F.; Gottschalk, A.; Mayer, G.; Heckel. *Angew. Chem., Int. Ed.* **2012**, *51*, 8446−8476.

(14) Szymański, W.; Beierle, J. M.; Kistemaker, H. A. V.; Velema, W. A.; Feringa, B. L. *Chem. Rev.* **2013**, *113*, 6114−6178.

(15) Irie, M. *Chem. Rev.* **2000**, *100*, 1685−1716.

(16) Matsuda, K.; Irie, M. *J. Photochem. Photobiol. C* **2004**, *5*, 169−182.

(17) Tian, H.; Yang, S. *Chem. Soc. Rev.* **2004**, *33*, 85−97.

(18) Yun, C.; You, J.; Kim, J.; Huh, J.; Kim, E. *J. Photochem. Photobiol. C* **2009**, *10*, 111−129.

(19) Beharry, A. A.; Sadovski, O.; Woolley, G. A. *J. Am. Chem. Soc.* **2011**, *133*, 19684−19687.

(20) Bléger, D.; Schwarz, J.; Brouwer, A. M.; Hecht, S. *J. Am. Chem. Soc.* **2012**, *134*, 20597−20600.

(21) Jukes, R. T. F.; Adamo, V.; Hartl, F.; Belser, P.; De Cola, L. *Inorg. Chem.* **2004**, *43*, 2779−2792.

(22) Indelli, M. T.; Carli, S.; Ghirotti, M.; Chiorboli, C.; Ravaglia, M.; Garavelli, M.; Scandola, F. *J. Am. Chem. Soc.* **2008**, *130*, 7286−7299.

(23) Fukaminato, T.; Doi, T.; Tanaka, M.; Irie, M. *J. Phys. Chem. C* **2009**, *113*, 11623−11627.

(24) Murata, R.; Yago, T.; Wakasa, M. *Bull. Chem. Soc. Jpn.* **2011**, *84*, 1336−1338.

(25) Mori, K.; Ishibashi, Y.; Matsuda, H.; Ito, S.; Nagasawa, Y.; Nakagawa, H.; Uchida, K.; Yokojima, S.; Nakamura, S.; Irie, M.; Miyasaka, H. *J. Am. Chem. Soc.* **2011**, *133*, 2621−2625.

(26) Carling, C.-J.; Boyer, J.-C.; Branda, N. R. *J. Am. Chem. Soc.* **2009**, *131*, 10838−10839.

(27) Osuka, A.; Fujikane, D.; Shinmori, H.; Kobatake, S.; Irie, M. *J. Org. Chem.* **2001**, *66*, 3913−3923.

(28) Kawai, T.; Sasaki, T.; Irie, M. *Chem. Commun.* **2001**, 711−712.

(29) Bens, A. T.; Frewert, D.; Kodatis, K.; Kryschi, C.; Martin, H.-D.; Trommsdorff, H. P. *Eur. J. Org. Chem.* **1998**, 2333−2338.

(30) Herrmann, A.; Müllen, K. *Chem. Lett.* **2006**, *35*, 978−985.

(31) Zhan, X.; Facchetti, A.; Barlow, S.; Marks, T. J.; Ratner, M. A.; Wasielewski, M. R.; Marder, S. R. *Adv. Mater.* **2011**, *23*, 268−284.

(32) Fukaminato, T.; Umemoto, T.; Iwata, Y.; Yokojima, S.; Yoneyama, M.; Nakamura, S.; Irie, M. *J. Am. Chem. Soc.* **2007**, *129*, 5932−5938.

(33) Tanifuji, N.; Irie, M.; Matsuda, K. *J. Am. Chem. Soc.* **2005**, *127*, 13344−13353.

(34) Odo, Y.; Matsuda, K.; Irie, M. *Chem.—Eur. J.* **2006**, *12*, 4283−4288.

(35) Aubert, V.; Ishow, E.; Ibersiene, F.; Boucekkine, A.; Williams, J. A. G.; Toupet, L.; Métivier, R.; Nakatani, K.; Guerchais, V.; Le Bozec, H. *New J. Chem.* **2009**, *33*, 1320−1323.

(36) Turro, N. J.; Ramamurthy, V.; Scaiano, J. C. Chapter 6: A Theory of Molecular Organic Photochemistry. In *Principles of Molecular Photochemistry: An Introduction*; University Science Books: Sausalito, CA, 2009; pp 319−382.

(37) Huang, P.-Y.; Chen, L.-H.; Chen, Y.-Y.; Chang, W.-J.; Wang, J.-J.; Lii, K.-H.; Yan, J.-Y.; Ho, J.-C.; Lee, C.-C.; Kim, C.; Chen, M.-C. *Chem.—Eur. J.* **2013**, *19*, 3721−3728.

(38) Rajasingh, P.; Cohen, R.; Shirman, E.; Shimon, L. J. W.; Rybtchinski, B. *J. Org. Chem.* **2007**, *72*, 5973−5979.

(39) Holman, M. W.; Liu, R.; Adams, D. M. *J. Am. Chem. Soc.* **2003**, *125*, 12649−12654.

(40) Langhals, H.; Karolin, J.; Johansson, L. B.-Å. *J. Chem. Soc. Faraday Trans.* **1998**, *94*, 2919−2922.

(41) *Gaussian 09*, Revision C.01, Frisch, M. J.; Trucks, G. W.; Schlegel, H. B.; Scuseria, G. E.; Robb, M. A.; Cheeseman, J. R.; Scalmani, G.; Barone, V.; Mennucci, B.; Petersson, G. A.; Nakatsuji, H.; Caricato, M.; Li, X.; Hratchian, H. P.; Izmaylov, A. F.; Bloino, J.; Zheng, G.; Sonnenberg, J. L.; Hada, M.; Ehara, M.; Toyota, K.; Fukuda, R.; Hasegawa, J.; Ishida, M.; Nakajima, T.; Honda, Y.; Kitao, O.; Nakai, H.; Vreven, T.; Montgomery, Jr., J. A.; Peralta, J. E.; Ogliaro, F.; Bearpark, M.; Heyd, J. J.; Brothers, E.; Kudin, K. N.; Staroverov, V. N.; Keith, T.; Kobayashi, R.; Normand, J.; Raghavachari,

K.; Rendell, A.; Burant, J. C.; Iyengar, S. S.; Tomasi, J.; Cossi, M.; Rega, N.; Millam, J. M.; Klene, M.; Knox, J. E.; Cross, J. B.; Bakken, V.; Adamo, C.; Jaramillo, J.; Gomperts, R.; Stratmann, R. E.; Yazyev, O.; Austin, A. J.; Cammi, R.; Pomelli, C.; Ochterski, J. W.; Martin, R. L.; Morokuma, K.; Zakrzewski, V. G.; Voth, G. A.; Salvador, P.; Dannenberg, J. J.; Dapprich, S.; Daniels, A. D.; Farkas, O.; Foresman, J. B.; Ortiz, J. V.; Cioslowski, J.; Fox, D. J.; Gaussian, Inc.: Wallingford, CT, 2010.